

Fragmentation of the valence states of CF_2Cl_2^+ , CF_2H_2^+ , and CF_2Br_2^+ studied by threshold photoelectron–photoion coincidence spectroscopy

Seccombe, Dominic; Tuckett, Richard; Fisher, B. O.

DOI:

[10.1063/1.1344889](https://doi.org/10.1063/1.1344889)

License:

Other (please specify with Rights Statement)

Document Version

Publisher's PDF, also known as Version of record

Citation for published version (Harvard):

Seccombe, D, Tuckett, R & Fisher, BO 2001, 'Fragmentation of the valence states of CF_2Cl_2^+ , CF_2H_2^+ , and CF_2Br_2^+ studied by threshold photoelectron–photoion coincidence spectroscopy', *Journal of Chemical Physics*, vol. 114, no. 9, pp. 4074-. <https://doi.org/10.1063/1.1344889>

[Link to publication on Research at Birmingham portal](#)

Publisher Rights Statement:

Fragmentation of the valence states of CF_2Cl_2^+ , CF_2H_2^+ , and CF_2Br_2^+ studied by threshold photoelectron–photoion coincidence spectroscopy

D. P. Seccombe and R. P. Tuckett

School of Chemistry, University of Birmingham, Edgbaston, Birmingham B152TT, United Kingdom

B. O. Fisher

Department of Physics, University of Reading, Whiteknights, Reading RG62AF, United Kingdom

The Journal of Chemical Physics 2001 114:9, 4074-4088

<http://aip.scitation.org/doi/10.1063/1.1344889>

General rights

Unless a licence is specified above, all rights (including copyright and moral rights) in this document are retained by the authors and/or the copyright holders. The express permission of the copyright holder must be obtained for any use of this material other than for purposes permitted by law.

- Users may freely distribute the URL that is used to identify this publication.
- Users may download and/or print one copy of the publication from the University of Birmingham research portal for the purpose of private study or non-commercial research.
- User may use extracts from the document in line with the concept of 'fair dealing' under the Copyright, Designs and Patents Act 1988 (?)
- Users may not further distribute the material nor use it for the purposes of commercial gain.

Where a licence is displayed above, please note the terms and conditions of the licence govern your use of this document.

When citing, please reference the published version.

Take down policy

While the University of Birmingham exercises care and attention in making items available there are rare occasions when an item has been uploaded in error or has been deemed to be commercially or otherwise sensitive.

If you believe that this is the case for this document, please contact UBIRA@lists.bham.ac.uk providing details and we will remove access to the work immediately and investigate.

Fragmentation of the valence states of CF_2Cl_2^+ , CF_2H_2^+ , and CF_2Br_2^+ studied by threshold photoelectron-photoion coincidence spectroscopy

D. P. Seccombe^{a)} and R. P. Tuckett^{b)}

School of Chemistry, University of Birmingham, Edgbaston, Birmingham B15 2TT, United Kingdom

B. O. Fisher

Department of Physics, University of Reading, Whiteknights, Reading RG6 2AF, United Kingdom

(Received 8 August 2000; accepted 8 December 2000)

Using tunable vacuum-ultraviolet radiation from a synchrotron, the decay pathways of the valence electronic states of CF_2X_2^+ ($\text{X}=\text{Cl}, \text{H}, \text{Br}$) in the range 10–25 eV have been determined by threshold photoelectron-photoion coincidence spectroscopy. The ions are separated by a linear time-of-flight mass spectrometer. Coincidence spectra are recorded continuously as a function of energy, allowing threshold photoelectron spectra and yields of the fragment ions to be obtained. At fixed photon energies, spectra are recorded with improved time resolution, allowing the mean total translational kinetic energy, $\langle \text{KE} \rangle_t$, into some dissociation channels to be determined. By comparing the $\langle \text{KE} \rangle_t$ values for single-bond fragmentations with those predicted for the limiting extremes of a statistical and an impulsive dissociation, information on the nature of the photodissociation dynamics can be inferred. The excited states of all three parent cations show some evidence for isolated-state behavior. With CF_2Cl_2^+ and CF_2H_2^+ , this is apparent from the form of the ion yields in the range 11–15 eV, whereas interpretation of the yields for CF_2Br_2^+ is hampered by an absence of thermochemical data. New upper limits at 298 K for the enthalpies of formation of CF_2H^+ ($593 \pm 3 \text{ kJ mol}^{-1}$) and CF_2Br^+ ($570 \pm 9 \text{ kJ mol}^{-1}$) are obtained. At higher photon energies, smaller fragment ions are formed following cleavage of more than one bond. With CF_2Cl_2 and CF_2Br_2 , the appearance energies of the fragment ions are close to the thermochemical energy for production of that ion with neutral atoms, suggesting that these ions form by bond-fission processes only. With CF_2H_2 , the one ion unambiguously assigned, CFH^+ , can only form at certain energies with molecular neutral fragments (i.e., $\text{CFH}^+ + \text{HF}$), involving simultaneous bond-breaking and bond-making processes. The $\langle \text{KE} \rangle_t$ values for cleavage of a single C–F or C–X bond suggest a relationship between the part of the molecule where ionization occurs and the bond that breaks; impulsive values of $\langle \text{KE} \rangle_t$ are more likely to be obtained when the breaking bond lies close to the part of the molecule from which ionization occurs, statistical values when ionization occurs further away from the breaking bond. Furthermore, for all CF_2X_2^+ cations there is a trend from impulsive to statistical behavior as the photon energy is increased. © 2001 American Institute of Physics. [DOI: 10.1063/1.1344889]

I. INTRODUCTION

In a recent publication,¹ a comprehensive study of the fragmentation of the outervalence states of CCl_3F^+ , CCl_3H^+ , and CCl_3Br^+ using coincidence techniques was presented. In this paper, coverage of the halo-substituted methanes is extended to the CF_2X_2^+ ($\text{X}=\text{Cl}, \text{H}, \text{Br}$) series where interest, like the previous study, derives from the fact that such molecules lie between the “small” and “large” molecule limits. A vacuum-ultraviolet (VUV) fluorescence study of these molecules found no evidence for parent ion emission,² indicating that the excited valence states of the parent ion primarily exhibit nonradiative decay processes such as dissociation into fragment ions. The fragmentation of

VUV-excited CF_2Cl_2^+ and CF_2H_2^+ has been extensively studied both by electron-impact mass spectrometry (EIMS) and photoionization mass spectrometry (PIMS),^{3–10} but studies have not been performed on CF_2Br_2^+ . The He I, and in some cases He II, photoelectron spectra of all three molecules have been measured by several groups,^{11–20} but no threshold photoelectron spectra (TPES) have been reported. TPES can be used to probe the effects of autoionization to near-threshold electrons in the titled molecules. In this paper, the TPES and the first threshold photoelectron-photoion coincidence (TPEPICO) study of the three molecules is presented, extending both the non-state-selective mass spectrometry studies^{3–10} and the work of Kischlat and Morgner who performed a few PEPICO experiments on CF_2Cl_2^+ using He I radiation as a photoexcitation source.²¹ The development of tunable VUV radiation from synchrotron sources has enabled the use of TPEPICO spectroscopy to provide state selectivity in the parent cation. Performed at sufficient

^{a)}Present address: Physics Department, The University, Newcastle-upon-Tyne, NE1 7RU, U.K.

^{b)}Author to whom correspondence should be addressed; electronic mail: r.p.tuckett@bham.ac.uk

mass resolution, the TPEPICO technique can also yield the total mean translational kinetic-energy release, $\langle \text{KE} \rangle_t$, into ionic dissociation channels. Thus, insight into the partitioning of energy into dissociation products may be gained. The aim of this work is to determine the identity of dominant fragmentation channels and the mechanism of dissociation of individual excited valence states of CF_2X_2^+ .

II. EXPERIMENT

Radiation in the range 10–30 eV from the 2 GeV synchrotron storage ring at the U.K. Daresbury Laboratory provides the tunable source of VUV radiation. The coincidence apparatus, comprising a threshold-energy electron analyzer and a linear time-of-flight (TOF) mass spectrometer, has been described in detail in previous publications.^{1,22,23} The two analyzers for electrons and ions are mounted colinearly within an evacuated stainless-steel chamber (base pressure = 5×10^{-8} Torr) attached to the storage ring of the synchrotron via a 1 m Seya–Namioka monochromator (best achievable resolution = 0.05 nm). One of two 1200 lines mm^{-1} gratings, mounted back to back inside the vacuum, can be used. The high-energy grating is used for most experiments where $\lambda < \sim 100$ nm ($E > 12.4$ eV), the medium-energy grating for $80 < \lambda < 120$ nm (10.3–15.5 eV). Sample gas is admitted into the vacuum chamber using a precision needle valve, operating pressures ranging from 1 to 5×10^{-5} Torr. Extraction of the electrons and ions from the interaction region through identical 20-mm-diam apertures is achieved by a 20 V cm^{-1} electrostatic field. The ions pass through a two-stage accelerating region configured to satisfy the first-order spatial focusing condition,²⁴ and a 182-mm-long field-free region. The threshold electrons are focused by a steriadancy analyzer onto the entrance slit of a 127° cylindrical postanalyzer, which serves primarily to remove on-axis energetic electrons. The mass-selected ions are detected by a pair of microchannel plates (Hamamatsu F4296-10), the threshold electrons by a channeltron (Phillips X818 BL). The amplified signals from both detectors can either be measured independently [for total ion yield or threshold photoelectron (TPE) spectroscopy] or in delayed coincidence (for TPEPICO spectroscopy). The two modes of operation occur simultaneously, using a dedicated personal computer (PC) equipped with a counter card and a purpose-built time-to-digital converter (TDC) card (Alan Burleigh of Pulsitron Ltd.). The best time resolution of the TDC card in its current configuration is 8 ns. CF_2H_2 and CF_2Cl_2 , manufactured by Aldrich and Fluorochem, respectively, were supplied in lecture bottles and used without further purification. CF_2Br_2 , from Aldrich, is a liquid at room temperature and pressure, and several freeze–thaw cycles were applied to it before use.

Measurements can be made either at fixed or varying photon energies. In the scanning-energy mode, flux-normalized TPEPICO, TPE, and total ion yield spectra are obtained in the range 10–25 eV. The VUV photon flux is monitored by measuring the fluorescence from a sodium salicylate window mounted behind the interaction region, using an EMI 9718 B photomultiplier tube in the dc mode. The scanning-energy TPEPICO spectrum accumulate as a three-dimensional histogram, where the coincidence count (color)

is plotted against photon energy and ion TOF. Given that only threshold electrons are detected, the photon energy is equivalent to the vibronic energy of CF_2X_2^+ above the ground state of CF_2X_2 , and the identity of the ions can readily be determined since their TOF depends on their mass and known parameters associated with the TOF mass spectrometer. Ion yields and breakdown diagrams are obtained by taking background-subtracted cross sections at values of the TOF corresponding to the observed ions. Appearance energies (AEs) of the parent and fragment ions can then be determined. At fixed energy, TPEPICO-TOF spectra are measured at a time resolution of 8 ns. Now, the coincidence count is plotted as a two-dimensional graph against the ion TOF. If the fragmentation is two bodied involving the fission of one bond only, a least-squares-fitting method is applied to the peak shape in order to determine the total mean-kinetic-energy release, $\langle \text{KE} \rangle_t$, into the two fragments.²⁵ This value can then be compared with those calculated using statistical, pure- and modified-impulsive models for dissociation. A full description of the theoretical models used for these dissociation mechanisms is given in Ref. 1.

III. ENERGETICS OF THE KEY DISSOCIATION CHANNELS

The energetics of the key dissociation channels ($\Delta_f H^0$ for $\text{CF}_2\text{X}_2 \rightarrow \text{A}^+ + n_1\text{B} + n_2\text{C} + e^-$, with $\text{X} = \text{Cl}, \text{H}, \text{Br}$, and $n_i = 0, 1, 2, 3$) and energies of the outervalence electronic states of the parent ions of CF_2X_2 are given in Table I. The thermochemical threshold, $\Delta_f H^0$, was determined by calculating the difference in the heats of formation ($\Delta_f H^0$) of products and reagents. The effects of internal energies are avoided if values for $\Delta_f H^0$ at 0 K are used. In cases where this was possible, values were taken from the JANAF tables.²⁶ For CF_2Br_2 and all of its ions except Br^+ , values of $\Delta_f H^0$ at 0 K were not available, hence, values at 298 K, taken from Lias *et al.*,²⁷ were used instead. We should note that the values for CCl_2F^+ (703 kJ mol^{-1}), CFCl^+ (1017 kJ mol^{-1}), CCl^+ (1243 kJ mol^{-1}), CF_2H^+ (611 kJ mol^{-1}), and CFH^+ (1121 kJ mol^{-1}) were obtained only by indirect methods.²⁷ No thermodynamic data are available for CF_2Br^+ , CFBr_2^+ , CFBr^+ , CF_2Br , and CFBr , so the thermochemistry of dissociation channels involving these fragments is unknown. Unless stated otherwise, the energies of the valence states of CF_2Cl_2^+ , CF_2H_2^+ , and CF_2Br_2^+ were taken from Cvitas, Gusten, and Klasinc,¹² Potts *et al.*,¹⁷ and Cvitas *et al.*,¹⁹ respectively.

The internal energies (E_{internal}) of CF_2Cl_2 and CF_2H_2 were calculated using the equation

$$E_{\text{internal}} = 1.5k_B T + \sum \frac{E_i}{\exp(E_i/k_B T) - 1}, \quad (1)$$

where $1.5k_B T$ is the contribution from the rotational degrees of freedom at temperature T , k_B is Boltzmann's constant, and E_i is the energy of the i th vibrational mode. The required vibrational frequencies were taken from the JANAF tables.²⁶ At 298 K, the internal energies for CF_2Cl_2 and CF_2H_2 were

TABLE I. Energetics of the key ionic dissociation channels and ionization energies of CF₂X₂ (X=Cl, H, Br).

Parent ion	Dissociation channel	Dissociation energy/eV	Adiabatic (vertical) IE/eV	Parent ion	Dissociation channel	Dissociation energy/eV	Adiabatic (vertical) IE/eV
CF ₂ Cl ₂ ⁺ $\tilde{H}^2B_1, \tilde{I}^2A_1$	CCl ₂ ⁺ +Cl+2F	20.77	(19.3)	CF ₂ H ₂ ⁺ \tilde{X}^2B_2	CFH ₂ ⁺ +F	14.02 ^d	12.729 ^a (13.29)
	CF ⁺ +2Cl+F	20.08			CF ₂ ⁺ +H ₂	13.88	
	CCl ₂ ⁺ +Cl+F ₂	19.17			CFH ⁺ +HF	13.38	
	CCl ₂ ⁺ +2F	18.70			CF ₂ H ⁺ +H	13.16 ^e	
	CCl ₂ ⁺ +F+FCI	18.21			Br ⁺ +C+2F+Br	27.08	
	CFCl ⁺ +Cl+F	17.63			Br ⁺ +C+Br+F ₂	25.48	
	CF ⁺ +Cl ₂ +F	17.60			Br ⁺ +C+FBr+F	24.54	
	CF ⁺ +FCI+Cl	17.52			Br ⁺ +CBr+2F	23.82	
	CCl ₂ ⁺ +F ₂	17.10					
	CF ₂ ⁺ +2Cl	16.82					
CF ₂ Cl ₂ ⁺ \tilde{G}^2A_1		16.90		CF ₂ Br ₂ ⁺ \tilde{K}^2A_1	Br ⁺ +CBr+F ₂	22.22	(22.5 ^f)
CF ₂ Cl ₂ ⁺ \tilde{F}^2A_2		16.30			Br ⁺ +CF+Br+F	21.52	
CF ₂ Cl ₂ ⁺ \tilde{E}^2B_1		15.90		CF ₂ Br ₂ ⁺ \tilde{J}^2B_2			(20.0 ^f)
	CFCl ⁺ +FCI	15.07		CF ₂ Br ₂ ⁺ \tilde{I}^2A_1			(19.0 ^f)
	CF ₂ ⁺ +Cl ₂	14.34			Br ⁺ +CF+FBr	18.97	
CF ₂ Cl ₂ ⁺ \tilde{D}^2B_2			14.126 ^a (14.36)		CF ⁺ +2Br+F	18.92	
CF ₂ Cl ₂ ⁺ \tilde{C}^2A_1			(13.45)	CF ₂ Br ₂ ⁺ \tilde{H}^2B_1	CF ⁺ +Br ₂ +F	16.48	(18.69 ^f)
CF ₂ Cl ₂ ⁺ \tilde{B}^2A_2	CFCl ₂ ⁺ +F	13.13 ^b		CF ₂ Br ₂ ⁺ \tilde{G}^2A_1	CF ⁺ +FBr+Br	16.37	(16.37 ^f)
CF ₂ Cl ₂ ⁺ \tilde{A}^2B_1			13.078 ^a (13.11)		Br ⁺ +CFBr+F	Unknown	
	CF ₂ Cl ⁺ +Cl	11.76 ^c	(12.53)		Br ⁺ +CF ₂ +Br	16.23	
CF ₂ Cl ₂ ⁺ \tilde{X}^2B_2			11.734 ^a (12.26)		CFBr ⁺ +F+Br	Unknown	
CF ₂ H ₂ ⁺ \tilde{G}^2A_1			(23.9)	CF ₂ Br ₂ ⁺ $\tilde{E}^2A_2/\tilde{F}^2B_1$	CF ₂ ⁺ +2Br	15.66	(15.57 ^f)
	CF ⁺ +2H+F	21.62			Br ⁺ +CF ₂ Br	Unknown	
	CFH ⁺ +H+F	19.24			CFBr ⁺ +FBr	Unknown	
	CF ₂ ⁺ +2H	18.36			CF ₂ ⁺ +Br ₂	13.22	
CF ₂ H ₂ ⁺ \tilde{F}^2B_2			18.270 ^a (18.97)	CF ₂ Br ₂ ⁺ \tilde{D}^2B_2			(13.22 ^f)
CF ₂ H ₂ ⁺ \tilde{E}^2A_1			18.236 ^a (18.97)	CF ₂ Br ₂ ⁺ \tilde{C}^2A_1			(12.41 ^f)
CF ₂ H ₂ ⁺ \tilde{D}^2B_1			18.208 ^a (18.97)	CF ₂ Br ₂ ⁺ \tilde{B}^2A_2			(12.06 ^f)
	CF ⁺ +F+H ₂	17.14		CF ₂ Br ₂ ⁺ \tilde{A}^2B_1			(11.56 ^f)
	CF ⁺ +H+HF	15.75			CFBr ₂ ⁺ +F	Unknown ^g	(11.17 ^f)
CF ₂ H ₂ ⁺ \tilde{C}^2A_2			15.624 ^a (15.58)	CF ₂ Br ₂ ⁺ \tilde{X}^2B_2	CF ₂ Br ⁺ +Br	≤11.00 ^h	
CF ₂ H ₂ ⁺ \tilde{B}^2A_1			15.572 ^a (15.58)				
CF ₂ H ₂ ⁺ \tilde{A}^2B_1			14.611 ^a (15.25)				

^aReference 14.^b $\Delta_f H^0$ for CFCl₂⁺ was determined from the observation of a near-thermoneutral reaction: C₂H₅⁺+CF₂Cl₂→CCl₂F⁺+C₂H₅F (Ref. 28).^c $\Delta_f H^0$ for CF₂Cl⁺ was determined from the observation of a near-thermoneutral reaction: C₂H₅⁺+CF₂Cl₂→CF₂Cl⁺+C₂H₅Cl (Ref. 27).^d $\Delta_f H^0$ for CFH₂⁺ was calculated from observed ion–molecule reactions (Ref. 28).^e $\Delta_f H^0$ for CF₂H⁺ was calculated from observed ion–molecule reactions (Ref. 28 and 29).^fReference 19.^gAppearance energy of CFBr₂⁺ at 298 K is 14.9±0.2 eV (this work).^hAppearance energy of CF₂Br⁺ at 298 K is 11.0±0.05 eV (this work). This energy is assumed to be an upper limit to the enthalpy of this reaction.

calculated to be 0.09 and 0.05 eV, respectively. An equivalent calculation was not required for CF₂Br₂⁺ (see Sec. IVC 3).

IV. RESULTS

A. CF₂Cl₂

1. TPES

As described in the preceding paper,² the electronic configuration of CF₂Cl₂ is (3a₁)²(3a₂)²(3b₁)²(3b₂)²(4a₁)²(4a₂)²(4b₁)²(4b₂)², where the numbering scheme does not include core orbitals.³⁰ A TPES of CF₂Cl₂ was recorded from 11.8 to 24.5 eV on the high-energy grating [Fig. 1(a)]

at a resolution of 0.3 nm. Peaks are observed at 12.28, 12.55, 13.14, 13.45, 14.41, 16.24, 19.29, and 20.3 eV. The first seven peaks correspond to the formation of the \tilde{X} , \tilde{A} , \tilde{B} , \tilde{C} , \tilde{D} , ($\tilde{E}/\tilde{F}/\tilde{G}$), and (\tilde{H}/\tilde{I}) states of the parent ion. The values measured are in excellent agreement with the He I measurements of vertical ionization energies (IEs) reported by Cvitas, Gusten, and Klasinc.¹² It can be informative to compare the relative intensities of the peaks observed in the TPES and He I spectra. Since the latter are recorded with a fixed-energy photon source, only electrons arising from direct ionization are likely to be detected, i.e., $A+h\nu\rightarrow A^++e^-$. By contrast, the TPES is measured by scanning the energy of a continuum radiation source. Hence, in addition to direct ioniza-

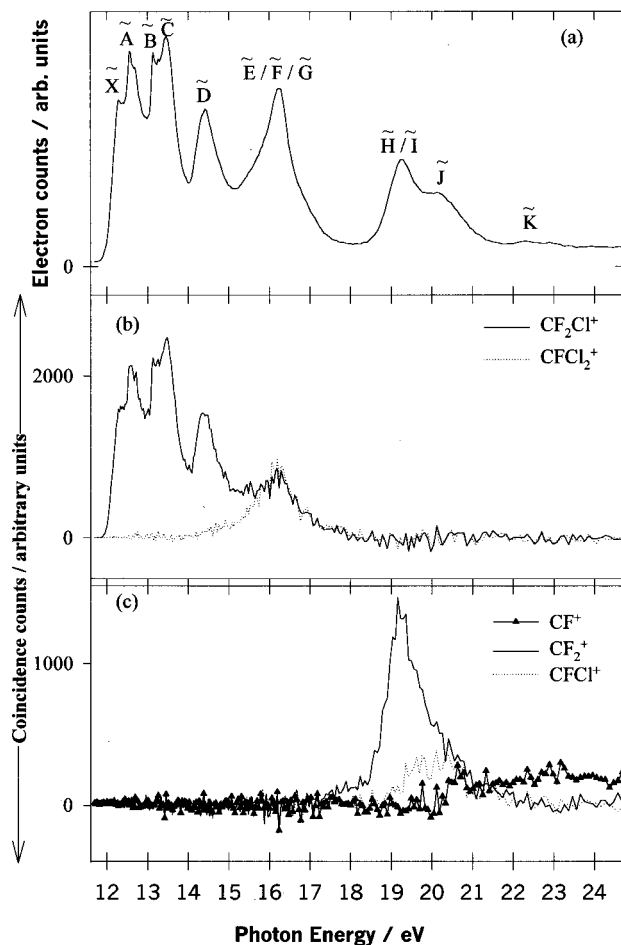


FIG. 1. (a) Threshold photoelectron spectrum of CF_2Cl_2 . The assignment of the electronic states of the parent ion (see Table I) is shown. (b) Coincidence ion yields of CF_2Cl^+ and CFCl_2^+ . (c) Coincidence ion yields of CF^+ , CF_2^+ , and CFCl^+ . The resolution of all spectra is 0.3 nm.

tion, electrons arising indirectly from autoionization processes will be detected provided their energy is close to 0 eV, i.e., $A + h\nu \rightarrow A^* \rightarrow A^+ + e^-$ (0 eV). Below 15 eV, the TPE and He I spectra of CF_2Cl_2 are quite similar, indicating that autoionization is not an important process; this assumes that the ionization cross sections are unchanged between threshold and 21.22 eV. In the TPES, the \tilde{A} state at 12.55 eV has a slightly low intensity while the \tilde{C} state at 13.45 eV has a slightly high intensity. These observations indicate that the effect of autoionization producing threshold-energy electrons among the lower valence states varies as $\tilde{C} > \tilde{X}$, \tilde{B} , $\tilde{D} > \tilde{A}$. Above 15 eV, the peaks in the threshold spectrum have a significantly higher relative intensity than those in the He I spectrum, indicating that autoionization is more important at these higher energies.

2. Scanning-energy TPEPICO experiments

The scanning-energy TPEPICO spectrum was also recorded from 11.8 to 24.5 eV at a photon resolution of 0.3 nm and an ion TOF resolution of 64 ns. While the fragment ions CF_2Cl^+ , CFCl_2^+ , CF_2^+ , CFCl^+ , and CF^+ are detected, neither the parent ion nor the fragments CCl^+ and CCl_2^+ are observed at any photon energy. Ion yields [Figs. 1(b) and

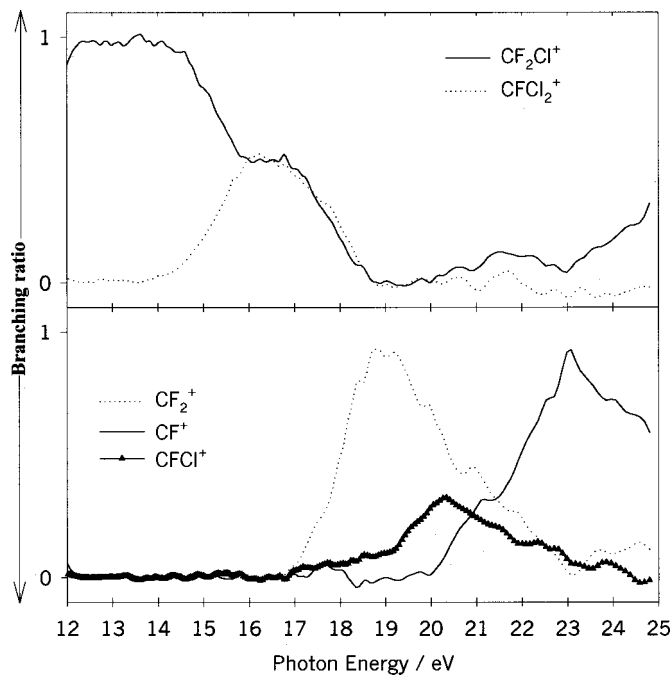


FIG. 2. Breakdown diagram for photofragmentation of CF_2Cl_2^+ .

1(c)] and breakdown diagrams (Fig. 2) were constructed by the method previously outlined. The \tilde{X} to \tilde{C} states fragment exclusively to CF_2Cl^+ , the \tilde{D} and $\tilde{E}/\tilde{F}/\tilde{G}$ states to CF_2Cl^+ and CFCl_2^+ , the \tilde{H}/\tilde{I} states to CF_2^+ , and the \tilde{J} state to CFCl^+ .

Appearance energies determined from the ion yields are given in Table II along with values obtained by EIMS or PIMS studies. The AE measured for CF_2Cl^+ , a sharp onset at 11.95 ± 0.05 eV, is in excellent agreement with previous PIMS measurements of Ajello, Huntress, and Rayerman,⁴ Jochims, Lohr, and Baumgärtel,⁵ and Schenk, Oertel, and Baumgärtel⁶ (11.99, 12.10, and 11.96 ± 0.03 eV, respectively). It should be noted, however, that the value quoted by Schenk, Oertel, and Baumgärtel⁶ is the higher of the two they quote. Their lower value, 11.81 eV, is assigned to the threshold energy for the process $\text{CF}_2\text{Cl}_2 \rightarrow \text{CF}_2\text{Cl}^+ + \text{F}^-$ and cannot, therefore, be compared with our study since ions without associated electrons cannot be detected in the TPEPICO experiment. Using electron-impact ionization, Baker and Tate³ determined an AE of 12.8 ± 0.2 eV, ~ 0.9 eV greater than the values obtained using photons. The discrepancy is probably due to the effect of the near-threshold Wannier law.³¹ We comment that it is now well established that due to secondary effects such as electron-ion recombination resulting in the variation of ionization cross section with energy close to threshold,³¹ energy thresholds are more accurately measured using photon sources. The thermochemical dissociation energy ($\Delta_r H^0$) is 11.76 eV (Table I). A comparison of this value with the AE is not meaningful since the oscillator strength associated with production of the parent ion is small below ~ 11.9 eV, the adiabatic ionization energy of CF_2Cl_2 being 11.73 eV.¹⁴ Since the lowest dissociation threshold ($\text{CF}_2\text{Cl}_2 \rightarrow \text{CF}_2\text{Cl}^+ + \text{Cl} + e^-$) lies at 11.76

TABLE II. Appearance energies of the ions formed following vacuum-UV photoexcitation of CF_2Cl_2 .

Fragment ion	Appearance Energies/eV				
	Baker <i>et al.</i> (EIMS) ^a	Ajello <i>et al.</i> (PIMS) ^b	Jochims <i>et al.</i> (PIMS) ^c	Schenk <i>et al.</i> (PIMS) ^d	This work (TPEPICO)
CCl^+	17.0±0.5			14.8±0.2 16.35±0.2 18.0±0.2 21.6±0.1	
CF^+	19.5±0.5		17.65 20.2	15.3±0.3 17.35±0.05 19.84±0.05	20.3±0.4
CFCl^+	18.1±0.2	17.76		15.2±0.3 17.50±0.05 18.60±0.05	18.7±0.3
CF_2^+	18.1±0.2	16.98	17.22	14.9±0.3 16.65±0.1	17.5±0.4
CFCl_2^+	15.4±0.2	13.81	14.15	13.30±0.05	14.2±0.3
CF_2Cl^+	12.8±0.2	11.99	12.10	11.81 11.96±0.03	11.95±0.05
CF_2Cl_2^+		11.75	11.75		

^aReference 3.^bReference 4.^cReference 5.^dReference 6.

eV, the majority of the Franck–Condon region of the $\text{CF}_2\text{Cl}_2^+ \tilde{X}^2B_2$ ground state is dissociative and, as a consequence, the parent ion is not detected.

The AE measured for CFCl_2^+ , a shallow onset at 14.2±0.3 eV, is in good agreement with the values of Ajello, Huntress, and Rayerman⁴ and Jochims, Lohr, and Baumgärtel,⁵ 13.81 and 14.15 eV, respectively. However, it is 1.2 eV lower than that of Baker and Tate,³ and significantly higher than the accurate measurement of Schenk, Oertel, and Baumgärtel, 13.30±0.05 eV.⁶ The value of Baker and Tate³ is probably high because electrons are used as the excitation source. The discrepancy with Schenk's measurement⁶ may be due to the possibility that CFCl_2^+ can also be produced by ion-pair formation ($\text{CF}_2\text{Cl}_2 \rightarrow \text{CFCl}_2^+ + \text{F}^-$; $\Delta_r H^0 = 9.27$ eV), although this process was not discussed. The thermochemical dissociation energy for $\text{CF}_2\text{Cl}_2 \rightarrow \text{CFCl}_2^+ + \text{F} + e^-$ is 13.13 eV, 1 eV lower than our value for the appearance energy. Under this circumstance it is pertinent to compare the two values since the oscillator strength associated with production of the parent ion is relatively high at 13.13 eV. Any barrier in an exit channel of a potential-energy surface involving a single-bond cleavage is likely to be much lower than 1 eV. Hence, it is thought that the 1 eV difference between the appearance energy and the thermochemical threshold arises from rapid nonstatistical fragmentation, between ~13 and 14 eV, of CF_2Cl_2^+ to CFCl_2^+ , following the removal of a Cl lone-pair electron. The same phenomenon was observed in the fragmentation of the lower valence states of CFCl_3^+ , resulting in an appearance energy for CCl_3^+ significantly higher than the value of $\Delta_r H^0$ associated with $\text{CFCl}_3 \rightarrow \text{CCl}_3^+ + \text{F} + e^-$.¹

The AE measured for CF_2^+ , a shallow onset at 17.5±0.4 eV, agrees acceptably with previous measurements. There are two possible channels for the formation of CF_2^+ : $\text{CF}_2\text{Cl}_2 \rightarrow \text{CF}_2^+ + \text{Cl}_2 + e^-$, $\Delta_r H^0 = 14.34$ eV, and $\text{CF}_2\text{Cl}_2 \rightarrow \text{CF}_2^+ + 2\text{Cl} + e^-$, $\Delta_r H^0 = 16.82$ eV. Comparison with the AE indicates that CF_2^+ is probably formed by the higher-energy process. It should be noted, however, that Schenk, Oertel, and Baumgärtel⁶ report two experimental values, 14.9±0.3 and 16.65±0.1 eV, the lower of which is attributed to $\text{CF}_2\text{Cl}_2 \rightarrow \text{CF}_2^+ + \text{Cl}_2 + e^-$. Since the process is not detected by the TPEPICO experiment, the lower AE probably arises from ion-pair formation, $\text{CF}_2\text{Cl}_2 \rightarrow \text{CF}_2^+ + \text{Cl}^- + \text{Cl}$, $\Delta_r H^0 = 13.23$ eV. The AE measured by us for CFCl^+ production, 18.7±0.3 eV, is significantly higher than any of the previous measurements, apart from Schenk, Oertel, and Baumgärtel,⁶ whose highest of three values is 18.60±0.05 eV. It is likely that below ~18.6 eV, the PIMS experiments of Schenk, Oertel, and Baumgärtel⁶ were detecting CFCl^+ produced by ion-pair dissociation processes. Indeed, they attribute their lower two AEs, at 15.2±0.3 and 17.50±0.05 eV, to $\text{CF}_2\text{Cl}_2 \rightarrow \text{CFCl}^+ + (\text{F}^-)^* + \text{Cl}$ and $\text{CF}_2\text{Cl}_2 \rightarrow \text{CFCl}^+ + \text{F} + (\text{Cl}^-)^*$, respectively. The AE measured by the TPEPICO experiment, 18.7±0.3 eV, is significantly higher than the thermochemical dissociation energies associated with the two possible dissociation channels, $\text{CFCl}^+ + \text{F} + \text{Cl} + e^-$ at 17.63 eV and $\text{CFCl}^+ + \text{FCl} + e^-$ at 15.07 eV. Hence, the likely dominant reaction cannot be determined.

The ion yield for CF^+ has poor statistics. The AE of 20.3±0.4 eV is in reasonable agreement with that given by Baker and Tate,³ 19.5±0.5 eV, and higher values obtained

TABLE III. Mean translational KE releases, $\langle \text{KE} \rangle_t$, of the two-body fragmentation of the valence states of CF_2Cl_2^+ .

Parent ion state	Fragment ion	E/eV	$\langle \text{KE} \rangle_t$ /eV	E_{avail} /eV ^a	Fraction ^b			
					Expt.	Statistical	Pure impulsive	Modified impulsive
\tilde{X}^2B_2	CF_2Cl^+	12.28	0.27 ± 0.04	0.61	0.44	0.17	0.36	0.36–0.87
\tilde{A}^2B_1	CF_2Cl^+	12.56	0.40 ± 0.05	0.89	0.45	0.16	0.36	0.36–0.87
\tilde{B}^2A_2	CF_2Cl^+	13.19	0.56 ± 0.05	1.52	0.37	0.15	0.36	0.36–0.87
\tilde{C}^2A_1	CF_2Cl^+	13.48	0.64 ± 0.05	1.81	0.35	0.15	0.36	0.36–0.87
\tilde{D}^2B_2	CF_2Cl^+	14.42	0.60 ± 0.03	2.75	0.22	0.14	0.36	0.36–0.87
$\tilde{E}/\tilde{F}/\tilde{G}$	CF_2Cl^+	16.25	0.60 ± 0.03	4.58	0.13	0.13	0.36	0.36–0.87
$\tilde{E}/\tilde{F}/\tilde{G}$	CFCl_2^+	16.25	1.1 ± 0.1	3.21	0.34	0.13	0.46	0.46–0.91

^a E_{avail} = photon energy(E) – thermochemical threshold for forming the daughter ion + thermal energy of the parent molecule at 298 K.

^bGiven by $\langle \text{KE} \rangle_t / E_{\text{avail}}$.

by Jochims, Lohr, and Baumgärtel,⁵ and Schenk, Oertel, and Baumgärtel,⁶ 20.2 and 19.84 ± 0.05 eV, respectively. Our AE agrees within error limits with the dissociation energy for the reaction which forms atomic products ($\text{CF}_2\text{Cl}_2 \rightarrow \text{CF}^+ + \text{F} + 2\text{Cl} + e^-$) and it, therefore, seems likely that this is the dominant dissociation channel. It is likely that the lower AEs that Jochims, Lohr, and Baumgärtel⁵ and Schenk, Oertel, and Baumgärtel⁶ report are due to ion-pair processes. Although the CCl^+ ion has been observed in both EIMS and PIMS experiments, the TPEPICO data presented here have failed to detect it. This is due either to a relative lack of sensitivity associated with the TPEPICO experiment, or that the CCl^+ ions detected in the EIMS experiments are only formed by ion-pair processes.

3. Fixed-energy TPEPICO experiments

TPEPICO-TOF spectra were measured for $\text{CF}_2\text{Cl}_2^+ \rightarrow \text{CF}_2\text{Cl}^+ + \text{Cl}$ at energies of 12.28, 12.56, 13.19, 13.48, 14.42, and 16.25 eV, corresponding to initial formation of the \tilde{X} , \tilde{A} , \tilde{B} , \tilde{C} , \tilde{D} , and $\tilde{E}/\tilde{F}/\tilde{G}$ states of the parent ion. In addition, a TPEPICO-TOF spectrum was recorded for $\text{CF}_2\text{Cl}_2^+ \rightarrow \text{CFCl}_2^+ + \text{F}$ at 16.25 eV. Experimental values for $\langle \text{KE} \rangle_t$ and $\langle f \rangle_t$ (defined as the fraction of the available energy released into translational energy of the products), and values of $\langle f \rangle_t$ determined for the statistical, pure-impulsive, and modified-impulsive cases, are given in Table III. Allowance has been made in the fitting procedure for the fact that each Cl atom exists as two isotopomers (³⁵Cl 75%, ³⁷Cl 25%).²⁵ The statistical fractions were calculated using known vibrational frequencies for the ν_1 (1507 and 1352 cm^{-1} for CF_2Cl^+ and CFCl_2^+ , respectively) and ν_5 (1406 and 1142 cm^{-1} , respectively) modes.³² The vibrational frequencies of the other four modes are unknown, so values for the isoelectronic BF_2Cl and BFCl_2 molecules were used.²⁶ The maximum values of $\langle f \rangle_t$ determined for the modified-impulsive model were calculated assuming that the polyatomic fragment (CF_2Cl^+ or CFCl_2^+) initially has a regular tetrahedral structure with bond angles of 109.5°. The minimum values were obtained assuming planar geometry

with bond angles of 120°. In calculating $\langle f \rangle_t$ for both the pure- and modified-impulsive cases, isotopically averaged masses were used.

The values of $\langle \text{KE} \rangle_t$ and $\langle f \rangle_t$ determined for CF_2Cl^+ fit well to a pure-impulsive model below 13.5 eV, although the slightly high values of $\langle f \rangle_t$ calculated at photon energies of 12.28 and 12.56 eV may be indicative of a small contribution of modified-impulsive behavior. The $\langle \text{KE} \rangle_t$ determined for dissociation of $\text{CF}_2\text{Cl}_2^+ \tilde{D}^2B_2$ at 14.42 eV fits to a statistical/impulsive hybrid mechanism, while dissociation of $\text{CF}_2\text{Cl}_2^+ \tilde{E}^2B_1/\tilde{F}^2A_2/\tilde{G}^2A_1$ at 16.25 eV appears to be purely statistical. Overall, there is a transition from impulsive to statistical behavior as the photon energy increases. The $\langle \text{KE} \rangle_t$ determined for CFCl_2^+ fits more closely to a pure-impulsive than to a statistical model.

B. CF_2H_2

1. TPES

As described previously,^{2,14} the electronic configuration of CF_2H_2 in C_{2v} symmetry is $(2a_1)^2(1b_2)^2(3a_1)^2(2b_1)^2(1a_2)^2(4a_1)^2(3b_1)^2(2b_2)^2$, where the numbering scheme does not include core orbitals.¹² A TPES of CF_2H_2 was measured from 12.4 to 27.5 eV on the high-energy grating at a resolution of 0.3 nm [Figs. 3 and 4(a)]. Peaks were observed at 13.3, 15.5, 19.1, and 24.0 eV corresponding to the formation of the \tilde{X}^2B_2 , $\tilde{A}/\tilde{B}/\tilde{C}$, $\tilde{D}/\tilde{E}/\tilde{F}$, and \tilde{G}^2A_1 states of the parent ion. The resolution in our experiment was not sufficient to resolve some of the overlapping states. An additional peak in the TPES at 17.4 eV has not previously been observed. With this exception, the peak positions of the TPES are in good agreement with the He I data.^{14–17} The relative intensities of the TPES and He I spectra, however, differ significantly. In the He I spectrum of Potts *et al.*,¹⁷ the ratio of the intensities of the \tilde{X} , $\tilde{A}/\tilde{B}/\tilde{C}$ and $\tilde{D}/\tilde{E}/\tilde{F}$ features are $\sim 2:2:1$, while the same analysis of the TPES gives $\sim 1:4:2$. Thus, the intensities of the $\tilde{A}/\tilde{B}/\tilde{C}$ and $\tilde{D}/\tilde{E}/\tilde{F}$ features compared to that of the \tilde{X} peak are enhanced under threshold conditions. In addition, the band at 17.4 eV is not observed in the He I ex-

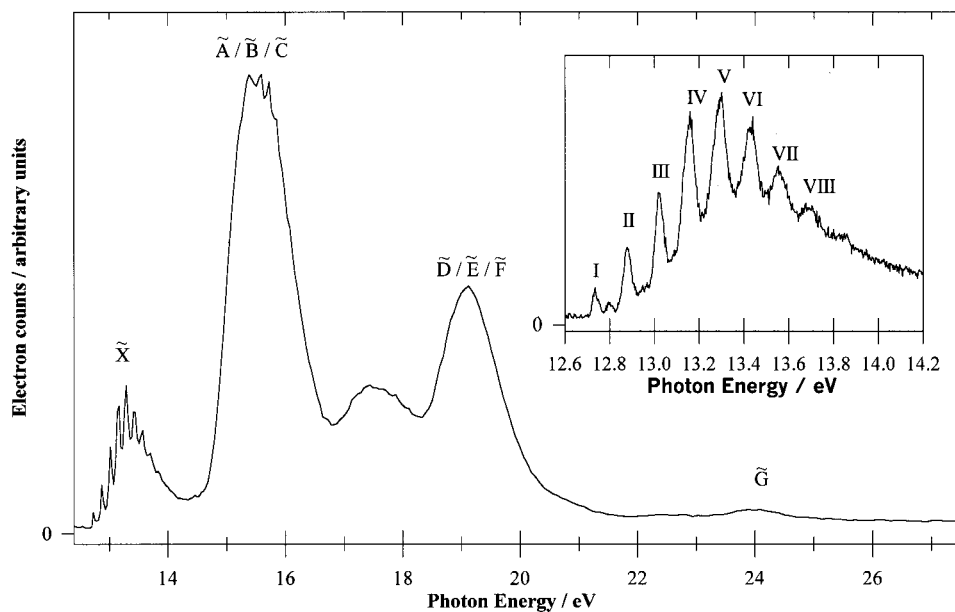


FIG. 3. Threshold photoelectron spectrum of CF_2H_2 . The resolution is 0.3 nm (main figure), 0.1 nm (inset). The assignment of the electronic states of the parent ion (see Table I) is shown.

periments. Hence, autoionization with the associated production of low-energy electrons appears to be an important process above ~ 14.5 eV, with its greatest effect in the range 17–18 eV.

A vibrationally resolved TPES was recorded for the \tilde{X}^2B_2 state from 12.6 to 14.0 eV with a resolution of 0.1 nm [Figs. 3 (inset) and 5(a)]. Several peaks are observed with a constant spacing of $1130 \pm 60 \text{ cm}^{-1}$. Peak positions and assignments are listed in Table IV, the values being in excellent agreement with those obtained by other groups at improved resolution.^{14,16} According to theory,³³ the extensive vibrational structure is caused mainly by a substantial reduction in the HCH bond angle upon ionization from 112° to 78° , with smaller changes in the FCF angle and the C–H and C–F bond lengths. The structure is, therefore, believed to

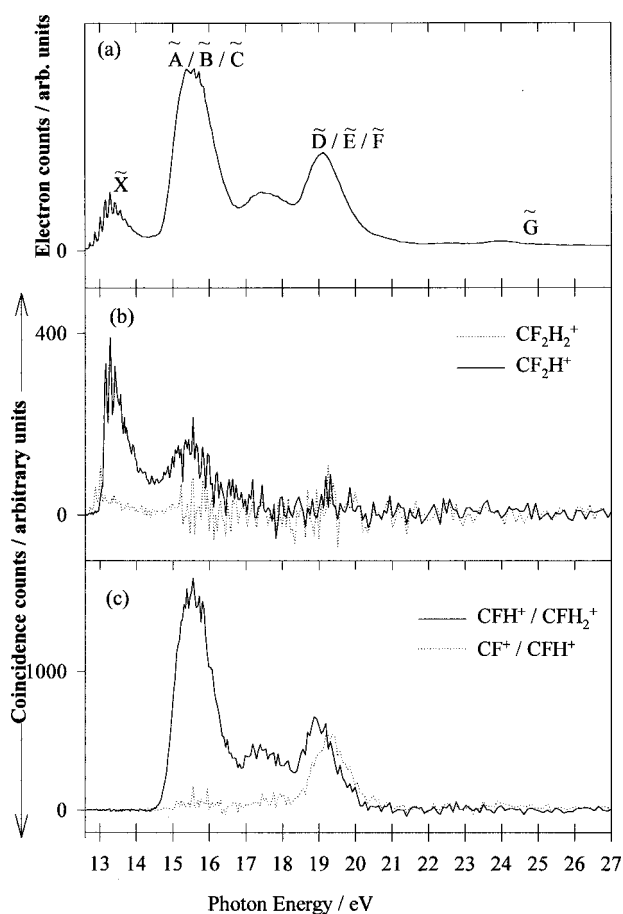


FIG. 4. (a) Threshold photoelectron spectrum of CF_2H_2 . (b) Coincidence ion yields of CF_2H_2^+ and CF_2H^+ . (c) Coincidence ion yields of $\text{CFH}^+/\text{CFH}_2^+$ and CF^+/CFH^+ . The resolution of all spectra is 0.3 nm.

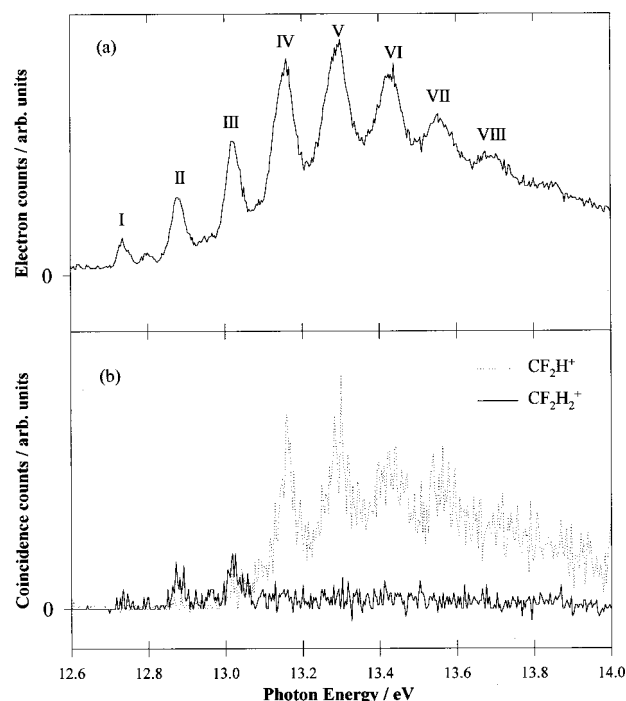


FIG. 5. (a) Threshold photoelectron spectrum of CF_2H_2 between 12.6 and 14.0 eV recorded at a resolution of 0.1 nm. (b) Coincidence ion yields for CF_2H_2^+ and CF_2H^+ recorded at the same resolution.

TABLE IV. Peak positions and assignments of the vibrational structure associated with the \tilde{X} state of CF_2H_2^+ .

Peak	Position/eV	Assignment
I	12.74	ν_2 and $\nu_3=0$
II	12.88	ν_2 or $\nu_3=1$
III	13.02	ν_2 or $\nu_3=2$
IV	13.16	ν_2 or $\nu_3=3$
V	13.30	ν_2 or $\nu_3=4$
VI	13.44	ν_2 or $\nu_3=5$
VII	13.55	ν_2 or $\nu_3=6$
VIII	13.70	ν_2 or $\nu_3=7$

arise from excitation of the near-degenerate ν_2 (CH_2 bend: a_1 symmetry) and ν_3 (C–F stretch: a_1 symmetry) modes. Calculations determine these ionic vibrational frequencies to be 1288 and 1412 cm^{-1} , respectively,³³ to be compared with experimental values of 1262 and 1116 cm^{-1} in the neutral ground state.³⁴ Pradeep and Shirley¹⁴ also invoke the presence of a third overlapping vibrational sequence in this photoelectron band, a $2\nu_4$ combination band (CF_2 bend: ν_4 having a_1 symmetry); the value of $2\nu_4$ in the neutral is 2×528 or 1056 cm^{-1} .³⁴ Although not relevant to our work, several groups have commented on the absence of vibrational structure in the $(2b_2)^{-1}\tilde{X}^2B_2$ photoelectron band of CF_2D_2 recorded at the same resolution as the CF_2H_2 spectrum.^{14,16} The most likely explanation for this behavior in CF_2D_2 is predissociation, causing a decrease in lifetime and, hence, a peak broadening.

2. Scanning-energy TPEPICO experiments

The scanning-energy TPEPICO spectrum was also measured from 12.4 to 27.5 eV at a photon resolution of 0.3 nm and an ion TOF resolution of 64 ns. Higher-resolution, fixed-energy TPEPICO-TOF spectra (Sec. IV B 3) reveal that the parent ion and fragment ions CF_2H^+ , CFH_2^+ , CFH^+ , and CF^+ are formed. The presence of two hydrogen atoms, and hence, the relatively small change in ion TOF following the loss of one or more hydrogen atom, renders the construction of ion yields difficult. Nevertheless, two unambiguous plots for CF_2H_2^+ and CF_2H^+ [Fig. 4(b)], and two composite plots for $\text{CFH}^+/\text{CFH}_2^+$ and CF^+/CFH^+ [Fig. 4(c)] have been constructed. By comparison with our study of CCl_3H where a similar problem occurs,¹ it seems likely that the dominant components of the two composite plots are CFH_2^+ and CFH^+ , involving the fission of one and two bonds, respectively. Assuming this to be true, AEs for CF_2H^+ , CFH_2^+ , and CFH^+ could be determined. They are listed in Table V, along with values reported by EIMS studies. The ion yields show that the \tilde{X}^2B_2 state of the parent ion is either stable or dissociates to CF_2H^+ , the $\tilde{A}/\tilde{B}/\tilde{C}$ states dissociate predominantly to CF_2H^+ and CFH_2^+ , and the $\tilde{D}/\tilde{E}/\tilde{F}$ states form predominantly CFH_2^+ and CFH^+ . A scanning-energy TPEPICO spectrum was also measured from 12.6 to 14.0 eV at a photon resolution of 0.1 nm and an ion TOF resolution of 64 ns. The time-of-flight range was adjusted so that only CF_2H_2^+ and CF_2H^+ could be detected, and ion yields [Fig. 5(b)] were determined. It can be seen that while the $\nu=0$ to

TABLE V. Appearance energies of the ions formed following vacuum–UV photoexcitation of CF_2H_2 .

Daughter ion	Appearance Energies/eV				
	Steele (EIMS) ^a	Lifshitz <i>et al.</i> (EIMS) ^b	Martin <i>et al.</i> (EIMS) ^c	Lossing (EIMS) ^d	This work (TPEPICO)
CF^+		18.8			
CF_2^+	14.8±0.4	20.7			
CFH^+		17.7			18.2±0.4
CFH_2^+		15.28		14.06	14.7±0.1
CF_2H^+		13.11	13.14±0.02	13.11	13.08±0.03
CF_2H_2^+		12.6			12.74±0.05

^aReference 7.

^bReference 8.

^cReference 9.

^dReference 10.

ν_2 or $\nu_3=2$ levels of the \tilde{X}^2B_2 state of CF_2H_2^+ are bound, the ν_2 or $\nu_3=3$ and higher vibrational levels dissociate to CF_2H^+ .

The AE measured for CF_2H^+ , 13.08 ± 0.03 eV, is in good agreement with previous measurements^{8–10} and the best determination to date of the thermochemical dissociation energy, $\Delta_r H^0 = 13.16$ eV. Our observations are consistent with the fact that lower vibrational levels of the ground state of the parent ion are bound. Assuming that the CF_2H^+ signal turns on at its thermochemical threshold, the AE can be used to refine the value for the 298 K enthalpy of formation of this fragment. Using values of $\Delta_f H_{298}^0$ for CF_2H_2 (-450.7 kJ mol⁻¹) and H (218.0 kJ mol⁻¹),²⁶ an upper limit for $\Delta_f H_{298}^0$ of CF_2H^+ is determined to be 593 ± 3 kJ mol⁻¹.

We commented above that the threshold in the $\text{CFH}^+/\text{CFH}_2^+$ ion yield [Fig. 4(c)] is likely to represent the AE for CFH_2^+ , rather than for CFH^+ . There are two reasons for this. First, since the former fragment requires fewer bonds to be broken, it is expected to appear at a lower energy. Second, the onset is sharp, implying that only one bond is broken. The AE determined for CFH_2^+ , 14.7 ± 0.1 eV, is ~ 0.7 eV above the appropriate thermochemical dissociation energy, 14.02 eV. We note that Lossing has reported an AE of 14.06 eV,¹⁰ in apparent contradiction to our work.

The threshold in the CF^+/CFH^+ ion yield plot is expected to give an AE for CFH^+ rather than CF^+ , since fewer bonds break to form the larger fragment. The AE determined for CFH^+ , 18.2 ± 0.4 eV, is in good agreement with the one previous measurement of Lifshitz and Long, 17.7 eV.⁸ Comparisons with the thermochemical data (Table I) indicate that close to the appearance energy CFH^+ must form with HF rather than with H+F. Although CF_2^+ has been detected in previous experiments, it was not observed in this TPEPICO study. Previous electron-impact measurements are contradictory. Steele⁷ reports a value of 14.8 ± 0.4 eV, while Lifshitz and Long⁸ obtain 20.7 eV. The former measurement indicates that CF_2^+ is probably formed with molecular hydrogen ($\Delta_r H^0 = 13.88$ eV), the latter that $\text{CF}_2\text{H}_2 \rightarrow \text{CF}_2^+ + 2\text{H} + e^-$ ($\Delta_r H^0 = 18.36$ eV) is likely to be the dominant dissociation channel. Unfortunately, our TPEPICO measurements are unable to resolve this discrepancy. On the other hand, CF^+ has been observed in our experiments (Sec. IV B 3), but

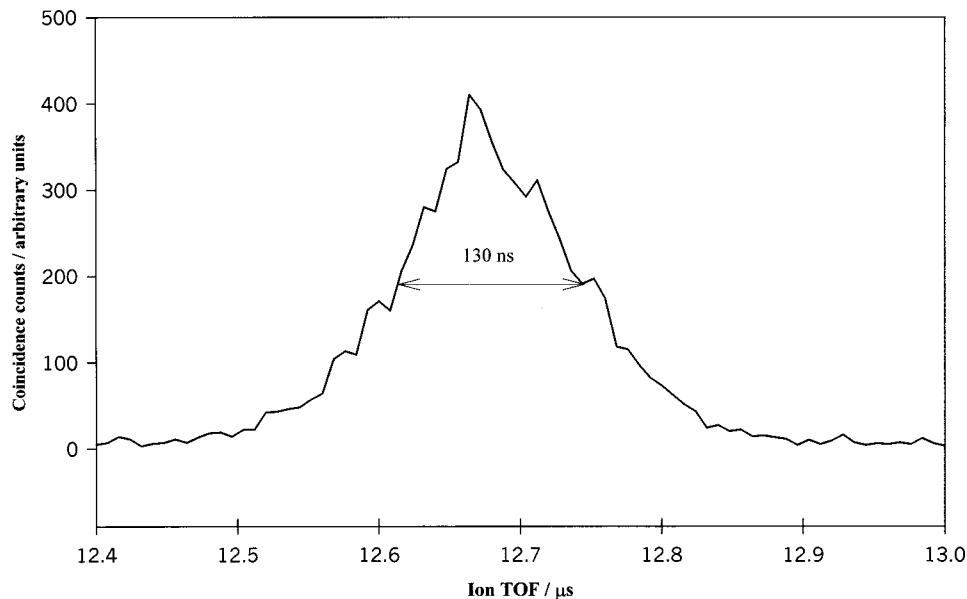


FIG. 6. TPEPICO-TOF spectrum of CF_2H_2 photoionized at 13.02 eV into the X^2B_2 (v_2 or $v_3=2$) state. The TOF resolution is 8 ns. The FWHM of the Gaussian peak is 130 ± 10 ns.

problems with mass resolution prevented its AE being determined accurately. It should be noted, however, that the AE obtained by us for CFH^+ , 18.2 ± 0.4 eV, is effectively a lower limit to the AE of CF^+ . Lifshitz and Long⁸ have reported an AE for CF^+ from CF_2H_2 of 18.8 eV. Of the three possible dissociation channels, only the two which form a neutral *molecular* product (HF or H_2) are thermodynamically allowed at this energy.

3. Fixed-energy TPEPICO experiments

TPEPICO-TOF spectra with a resolution of 8 ns were recorded at 12.74, 12.88, and 13.02 eV, energies which correspond to formation of the \bar{X}^2B_2 state of CF_2H_2^+ in its three lowest-observed vibrational levels. As excitation takes place below the first dissociation threshold, a peak at the TOF expected for the parent ion, 12.68 μs , is observed. The full width at half maximum (FWHM) of the parent ion peak measured at 13.02 eV was determined to be 130 ± 10 ns (Fig. 6). This value is in good agreement with that calculated for ions produced only with a thermal distribution of velocities at 298 K in an apparatus with an extraction field of 20 V cm^{-1} .³⁵ TPEPICO-TOF spectra were recorded at several photon energies between 13.16 and 15.69 eV, with the TOF range set so that only CF_2^+ , CF_2H^+ , and CF_2H_2^+ were detected. Only CF_2H^+ was observed. Unfortunately, values of $\langle \text{KE} \rangle_t$ for $\text{CF}_2\text{H}_2^+ \rightarrow \text{CF}_2\text{H}^+ + \text{H}$ could not be determined accurately due to unfavorable kinematics, since the CF_2H^+ fragment takes away only 2% of the kinetic energy released.

TPEPICO-TOF spectra were also recorded at a resolution of 8 ns for photon energies of 15.31, 15.69, and 17.46 eV [Fig. 7(a)]. The TOF range was set so that CF^+ , CFH^+ , and CFH_2^+ could all be detected. In this energy range only the larger of the three ions, with a peak center of 10.05 μs , was observed. Experimental values for $\langle \text{KE} \rangle_t$ and $\langle f \rangle_t$ were determined and, along with predicted statistical and impulsive values of $\langle f \rangle_t$, are listed in Table VI. Since only one of the vibrational frequencies was available for CFH_2^+ , $\nu_2 = 1450 \pm 30 \text{ cm}^{-1}$,³⁶ and none for the isoelectronic molecule

BFH_2 , the statistical fractions had to be calculated assuming that $\langle \text{KE} \rangle_{t \text{ stat}} \geq h\nu_i$. As the values predicted for $\langle \text{KE} \rangle_{t \text{ stat}}$ are quite large, this assumption is probably valid. The impulsive fractions were calculated using the assumptions given in Sec. IV A 3. At energies of 15.31 and 15.61 eV, the mechanism for dissociation of $\text{CF}_2\text{H}_2^+ \rightarrow \text{CFH}_2^+ + \text{F}$ seems to be predominantly impulsive (Table VI). Conversely, at the higher

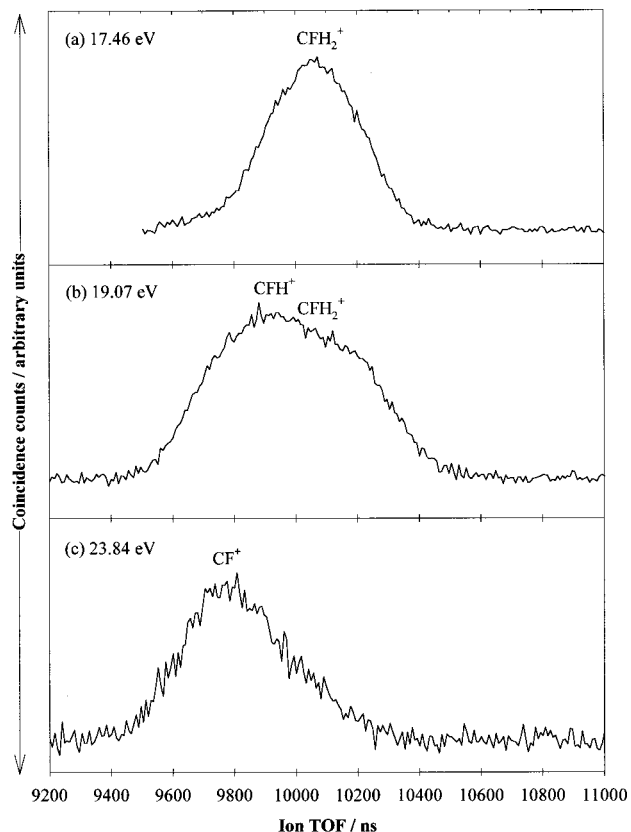


FIG. 7. TPEPICO-TOF spectra of (a) $\text{CFH}_2^+/\text{CF}_2\text{H}_2$ at 17.46 eV, (b) CFH^+ and $\text{CFH}_2^+/\text{CF}_2\text{H}_2$ at 19.07 eV, (c) $\text{CF}^+/\text{CF}_2\text{H}_2$ at 23.84 eV. In each case, the TOF resolution is 8 ns.

TABLE VI. Mean translational KE releases, $\langle \text{KE} \rangle$, of the two-body fragmentation of the valence states of CF_2H_2^+ .

Parent ion state	Daughter ion	E/eV	$\langle \text{KE} \rangle/\text{eV}$	$E_{\text{avail}}/\text{eV}^{\text{a}}$	Fraction ^b			
					Expt.	Statistical	Pure impulsive	Modified impulsive
\tilde{A}^2B_1	CFH_2^+	15.31	0.72 ± 0.04	1.34	0.54	$\sim 0.12^{\text{c}}$	0.61	0.61–0.68
\tilde{B}/\tilde{C}	CFH_2^+	15.69	0.78 ± 0.04	1.72	0.45	$\sim 0.12^{\text{c}}$	0.61	0.61–0.68
?	CFH_2^+	17.46	0.8 ± 0.1	3.49	0.23	$\sim 0.12^{\text{c}}$	0.61	0.61–0.68

^a E_{avail} = photon energy(E) – thermochemical threshold for forming the daughter ion + thermal energy of the parent molecule at 298K.

^bGiven by $\langle \text{KE} \rangle / E_{\text{avail}}$.

^cVibrational frequencies of CFH_2^+ and isoelectronic BFH_2 are unknown. Hence, calculation was performed assuming $\langle \text{KE} \rangle \gg h\nu_i$ for all vibrational modes.

energy of 17.46 eV, statistical behavior appears to dominate.

Finally, TPEPICO-TOF spectra were recorded at 19.07 and 23.84 eV, with the TOF range again set to observe CF^+ , CFH^+ , and CFH_2^+ [Figs. 7(b) and 7(c)]. The purpose of these measurements was not to extract dynamic information, but to determine the identity of the fragment ion. (By contrast with CF_2Cl_2 and CF_2Br_2 , it was not possible to obtain this information from fixed-energy cross sections of the scanning-energy TPEPICO spectra due to the large degree of overlap of the features.) From Fig. 7, it is clear that at 19.07 eV CFH_2^+ and CFH^+ are produced, while at 23.84 eV predominantly CF^+ , with a peak center of 9.79 μs , is formed.

C. CF_2Br_2

1. TPES

The electronic configuration of CF_2Br_2 is $(3a_1)^2(3a_2)^2(3b_1)^2(3b_2)^2(4a_1)^2(4a_2)^2(4b_1)^2(4b_2)^2$, where the numbering scheme does not include core orbitals.¹⁹ A TPES was recorded from 10 to 26 eV on both the high- and medium-energy gratings with a resolution of 0.3 nm [Fig. 8(a)], and the spectra were spliced together at 14 eV. Peaks are observed at 11.13, 11.57, 12.00, 12.35, 13.38, 15.55, 16.5, 18.8, and 20.0 eV, corresponding to formation of the \tilde{X} , \tilde{A} , \tilde{B} , \tilde{C} , \tilde{D} , \tilde{E}/\tilde{F} , \tilde{G} , \tilde{H}/\tilde{I} , and \tilde{J} states of the parent ion. All values are in good agreement with the He I and He II data of Cvitas *et al.*¹⁹ Below 15 eV, the appearance of the TPES is similar to that of the He I spectrum,¹⁹ except for a slight difference in the relative intensities of \tilde{X} and \tilde{A} peaks compared to the \tilde{B} , \tilde{C} , and \tilde{D} peaks. In the threshold spectrum this ratio is smaller, implying that autoionization is slightly more important for the higher excited states. Above 15 eV, the threshold spectrum shows a significant increase in the intensity of the peaks, as compared with the He I measurements. Hence, autoionization is prevalent in the valence states \tilde{E}^2A_2 through to \tilde{J}^2B_2 . This pattern is similar to that observed in both CF_2Cl_2 and CF_2H_2 .

2. Scanning-energy TPEPICO experiments

The scanning-energy TPEPICO spectrum was also measured from 10 to 26 eV at a photon resolution of 0.3 nm and an ion TOF resolution of 128 ns. Cross sections taken at

fixed photon energies reveal that over this range CF_2Br_2^+ , CF_2Br^+ , CFBr_2^+ , CF_2^+ , CFBr^+ , CF^+ , and Br^+ are formed. Br^+ is the only example observed in these TPEPICO studies of a non-carbon-containing ion. Ion yields [Figs. 8(b) and 8(c)] and breakdown curves (Fig. 9) were constructed. From the former, it can be seen that the \tilde{X}^2B_2 state of the parent ion either remains bound or dissociates to CF_2Br^+ via cleavage of the weakest C–Br bond. The low-lying states of CF_2Br_2^+ , \tilde{A}^2B_1 through to \tilde{D}^2B_2 , dissociate solely to CF_2Br^+ ; the near-degenerate \tilde{E}/\tilde{F} states form both CF_2Br^+ and CFBr_2^+ ; the \tilde{G}^2A_1 and \tilde{H}/\tilde{I} states form CF_2^+ and

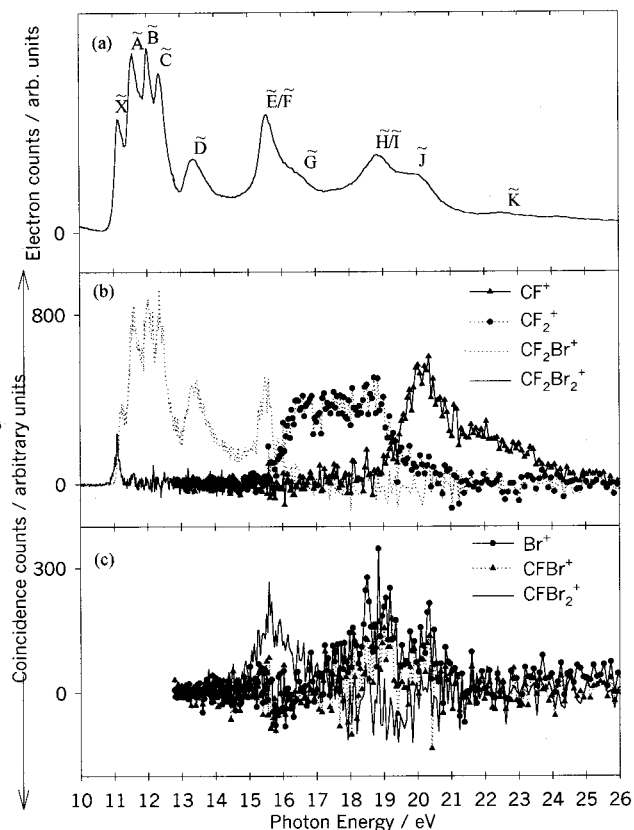


FIG. 8. (a) Threshold photoelectron spectrum of CF_2Br_2 . The assignment of the electronic states of the parent ion (see Table I) is shown. (b) Coincidence ion yields of CF_2Br_2^+ , CF_2Br^+ , CF_2^+ , and CF^+ . (c) Coincidence ion yields of CFBr_2^+ , CFBr^+ , and Br^+ . The resolution of all spectra is 0.3 nm.

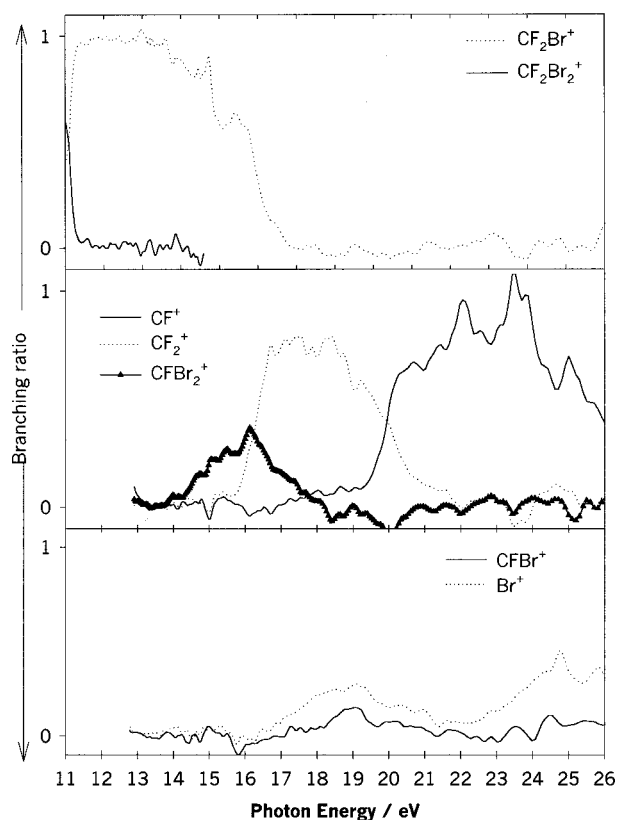


FIG. 9. Breakdown diagram for photofragmentation of CF_2Br_2^+ . The resolution of the spectrum is 0.3 nm.

CFBr^+ ; and the \tilde{J}^2B_2 and \tilde{K}^2A_1 states form CF^+ . In Table VII, AEs of these fragment ions determined for the first time from CF_2Br_2 are listed. With the exception of Br , Br^+ , and Br_2 , the thermochemistry for Br -containing fragments (e.g., CFBr_2^+) is not available (see Table I).

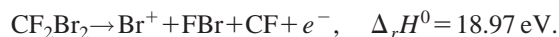
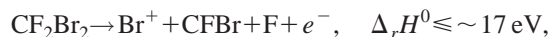
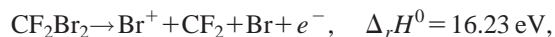
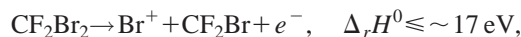
The AE of CF_2Br^+ is measured to be 11.00 ± 0.05 eV. The threshold for formation of this ion occurs within the Franck–Condon region of the \tilde{X}^2B_2 ground electronic state of the parent ion. This state clearly has a bound potential well. The exit channel for dissociation to $\text{CF}_2\text{Br}^+ + \text{Br}$ is unlikely to have any barrier, and there are no competing dissociation channels. It is reasonable, therefore, to use the AE of CF_2Br^+ to yield new thermodynamic information. The AE is an upper limit to $\Delta_r H_{298}^0$ of the reaction $\text{CF}_2\text{Br}_2 \rightarrow \text{CF}_2\text{Br}^+ + \text{Br} + e^-$. Since enthalpies of formation at 298 K for both Br and CF_2Br_2 are known, 112 and -379

TABLE VII. Appearance energies of the ions formed by vacuum–UV photoexcitation of CF_2Br_2 .

Daughter ion	Appearance energy/eV (TPEPICO)
CF^+	19.2 ± 0.4
CFBr^+	18.0 ± 0.5
Br^+	17.5 ± 0.5
CF_2^+	15.8 ± 0.3
CFBr_2^+	14.9 ± 0.2
CF_2Br^+	11.00 ± 0.05
CF_2Br_2^+	10.9 ± 0.05

± 8 kJ mol $^{-1}$, respectively,^{26,27} we can determine that $\Delta_r H_{298}^0(\text{CF}_2\text{Br}^+) \leq 570 \pm 9$ kJ mol $^{-1}$. In principle, using AEs for CFBr_2^+ and CFBr^+ , similar calculations can be performed to determine upper limits for the enthalpies of formation of these ions. Although technically correct, effects such as excitation into repulsive states, barriers along the exit channel of the potential-energy surface, and nonstatistical competition between dissociation channels may render the real thermodynamic values significantly lower than those calculated. Hence, these calculations were not performed.

The AE measured for CF_2^+ , 15.8 ± 0.3 eV, is very close to the thermochemical dissociation energy for forming CF_2^+ with two bromine atoms ($\Delta_r H^0 = 15.66$ eV), hence, this is likely to be the dominant dissociation channel. Similarly, the AE measured for CF^+ , 19.2 ± 0.4 eV, agrees, within error limits, with the dissociation energy associated with the formation of CF^+ with three atomic products ($\Delta_r H^0 = 18.92$ eV). For Br^+ , with an AE of 17.5 ± 0.5 eV, the situation is considerably more complicated since there are ten possible dissociation channels (Table I). In some cases there are likely to be large barriers along the exit channel of the potential-energy surface. In addition, dissociation energies for the two channels which involve CFBr and CF_2Br are unknown, although comparisons with similar reactions indicate that their values probably lie below ~ 17 eV. Over the range of energies where signal is observed, 17.5–21.0 eV, there are only four thermodynamically accessible dissociation channels:



Based on our previous experience of bulky molecules,¹ it is unlikely that any dissociation channel involving a barrier along the exit channel of the potential-energy surface plays a significant role. Hence, the final reaction can be discarded. Of the three other processes, it is not possible to decide which is dominant until, at the very least, the thermochemistry is known more accurately.

3. Fixed-energy TPEPICO experiments

The TPEPICO-TOF spectrum with an ion TOF resolution of 8 ns was measured at a photoexcitation energy of 11.12 eV, with the TOF range set to detect the parent ion (Fig. 10). The spectrum represents a superposition of the three isotopomers of CF_2Br_2 ($\text{CF}_2^{35}\text{Br}_2$ 25%, $\text{CF}_2^{35}\text{Br}^{37}\text{Br}$ 50%, $\text{CF}_2^{37}\text{Br}_2$ 25%), hence, its FWHM cannot be related simply to the width of a single Gaussian distribution.³⁵ Instead, the sum of three Gaussian functions is compared with the spectrum (Fig. 10), with each Gaussian representing one isotopomer of CF_2Br_2 . The individual functions are calculated from Franklin, Hierl, and Whan,³⁵ the heights being determined by the relative natural abundance, the TOF centers being determined by the mass of the isotopomer, and the

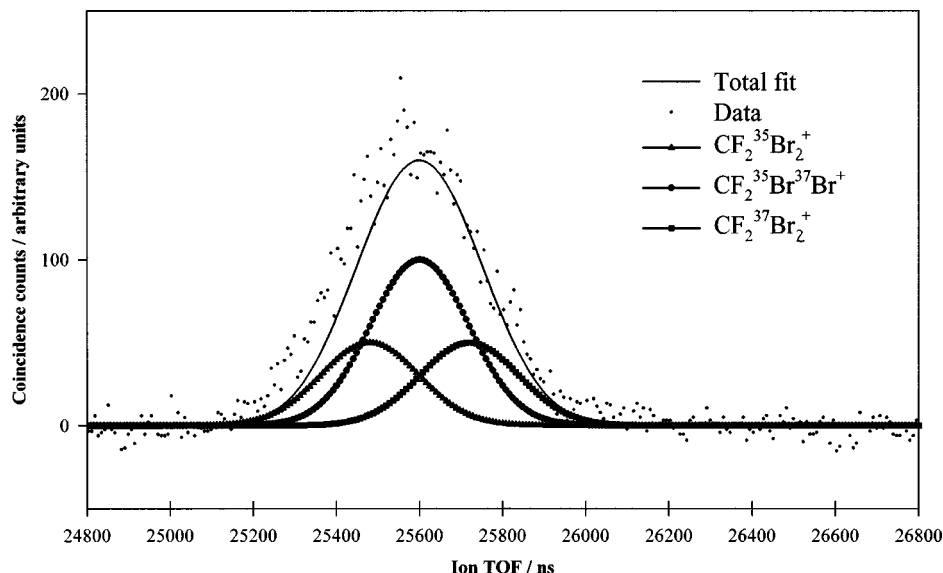


FIG. 10. TPEPICO-TOF spectrum of CF_2Br_2 photoionized at 11.12 eV into the X^2B_2 state of the parent ion. The TOF resolution is 8 ns. Gaussian peaks for each of the three isotopomers of CF_2Br_2 , with widths characterized by $T_{\text{trans}} = 298$ K and an extraction field of 20 V cm^{-1} (Ref. 35) have been added together and compared with the experimental data.

widths by the translational temperature and the extraction field. The total simulated feature fits reasonably to the raw data.

TPEPICO-TOF spectra were measured for CF_2Br^+ at photon energies of 11.12, 11.59, 11.99, 12.35, 13.33, and 15.50 eV, corresponding to initial formation of the \tilde{X} , \tilde{A} , \tilde{B} , \tilde{C} , \tilde{D} , and \tilde{E}/\tilde{F} states of the parent ion. A spectrum was also recorded for CFBr_2^+ at 15.50 eV, but unfavorable kinematics prevent the value of $\langle \text{KE} \rangle_t$ into $\text{CFBr}_2^+ + \text{F}$ from being determined accurately. Values of $\langle \text{KE} \rangle_t$ for the $\text{CF}_2\text{Br}_2^+ \rightarrow \text{CF}_2\text{Br}^+ + \text{Br}$ measurements have been determined and are listed in Table VIII. The fitting procedure allows for the fact that Br exists in two isotopic forms.²⁵ Since the thermochemistry of CF_2Br^+ was unknown, difficulties arose in calculating the excess energy and, hence, $\langle f \rangle_t$. For reasons discussed in the previous section, the AE of CF_2Br^+ , 11.00 ± 0.05 eV, is considered to be a good approximation to $\Delta_r H_{298}^0$ for $\text{CF}_2\text{Br}_2 \rightarrow \text{CF}_2\text{Br}^+ + \text{Br}$. Hence, the excess energy can be calculated by subtracting 11.00 eV from the photon energy; we note that it is not necessary to add the internal energy of CF_2Br_2 at 298 K to the value obtained for the excess energy, since the AE is a room-temperature measurement. Experimental values for $\langle f \rangle_t$, and those predicted for

the statistical and impulsive models, are given in Table VIII. The statistical fractions were calculated using known vibrational frequencies for the ν_1 and ν_2 modes of CF_2Br^+ , 1480 and 1362 cm^{-1} , respectively.³⁷ Vibrational frequencies of the other modes are unknown, hence, values determined for the isoelectronic molecule BF_2Br were used.²⁶ Fractions for the impulsive models were calculated using the assumptions outlined in Sec. IV A 3 and Ref. 1. Table VIII suggests that there is a general trend from modified-impulsive to statistical behavior as the photon energy is increased. It should be noted that the fractions calculated for the statistical and pure-impulsive models are quite similar, rendering the differentiation of these processes difficult. The value of $\langle f \rangle_t$ measured for the dissociation of the near-degenerate \tilde{E}/\tilde{F} states of CF_2Br_2^+ is extremely low, 0.07. This cannot be explained by any of the dissociation mechanisms.

V. DISCUSSION

A. Dissociation channels

A comparison of appearance energies of fragment ions with thermochemical thresholds can yield information about both the mechanism of dissociation and the identity of the

TABLE VIII. Mean translational KE releases, $\langle \text{KE} \rangle_t$, of the two-body fragmentation of the valence states of CF_2Br_2^+ .

Parent ion state	Daughter ion	E/eV	$\langle \text{KE} \rangle_t/\text{eV}$	$E_{\text{avail}}/\text{eV}^a$	Fraction ^b			
					Expt.	Statistical	Pure impulsive	Modified impulsive
\tilde{X}^2B_2	CF_2Br^+	11.12	0.06 ± 0.01	0.12	0.50	0.30	0.21	0.21–0.44
\tilde{A}^2B_1	CF_2Br^+	11.59	0.15 ± 0.03	0.59	0.25	0.17	0.21	0.21–0.44
\tilde{B}^2A_2	CF_2Br^+	11.99	0.23 ± 0.05	0.99	0.23	0.16	0.21	0.21–0.44
\tilde{C}^2A_1	CF_2Br^+	12.35	0.30 ± 0.05	1.35	0.22	0.15	0.21	0.21–0.44
\tilde{D}^2B_2	CF_2Br^+	13.33	0.32 ± 0.05	2.33	0.14	0.14	0.21	0.21–0.44
\tilde{E}/\tilde{F}	CF_2Br^+	15.50	0.33 ± 0.05	4.50	0.07	0.13	0.21	0.21–0.44

^a $E_{\text{avail}} = \text{Photon energy}(E) - \text{AE}_{298}(\text{CF}_2\text{Br}^+/\text{CF}_2\text{Br}_2)$, 11.00 eV.

^bGiven by $\langle \text{KE} \rangle_t / E_{\text{avail}}$.

dissociation channel. For fragment ions formed by the fission of one bond only, clearly there is a unique dissociation channel. For a pure statistical dissociation mechanism, the fraction of available energy released into translational kinetic energy of the two fragments is relatively small, with the fraction decreasing as the size of the fragments (and, hence, the number of available vibrational modes) increases. This is the case where the weakest C–X bond in CF_2X_2^+ breaks to form $\text{CF}_2\text{X}^+ + \text{X}$ (X=Cl, H, and Br). For an impulsive mechanism, where isolated-state behavior is observed in excited electronic states of the parent ion, the fraction of the available energy released into translational energy of the two fragments is greater than in a statistical dissociation. This appears to be the case when the stronger C–F bond in CF_2X_2^+ breaks to form $\text{CFX}_2^+ + \text{F}$. Due to unfavorable kinematics, this effect in the kinetic-energy release cannot be measured in $\text{CFBr}_2^+ + \text{F}$. It is, however, observed in $\text{CFH}_2^+ + \text{F}$ and, to a lesser extent, in $\text{CFCl}_2^+ + \text{F}$. Similar effects have been observed in previous TPEPICO photofragmentation studies of state-selected CCl_3X^+ (X=F, Cl, Br) and CF_3Y^+ (Y=Cl, Br).^{1,38}

For fragment ions formed by the fission of two or more bonds, necessarily, there exist more than one dissociation channel. Each has its own thermochemical threshold energy, hence, the identity of the dominant channel has a significant effect on the AE of the fragment. We have found that in many cases the dominant channel can be inferred by comparing values of $\Delta_r H^0$ with the AE of the fragment ion. In general, such dissociation channels conform to one of two limiting cases. The first, characterized by the absence of any barrier along the exit channel of the potential-energy surface, was found to occur in the dissociation of CCl_3F^+ and CCl_3Br^+ .¹ Processes involving bond fission only and loose transition states, such as $\text{CCl}_3\text{F} \rightarrow \text{CCl}^+ + 2\text{Cl} + \text{F} + e^-$ and simpler reactions such as $\text{CCl}_3\text{F} \rightarrow \text{CCl}_2\text{F}^+ + \text{Cl} + e^-$, fall into this category. The second, characterized by a large barrier along the exit channel, was shown to occur to some extent in the dissociation of CCl_3H^+ .¹ Processes where bond breaking occurs simultaneously with bond formation, e.g., $\text{CCl}_3\text{H} \rightarrow \text{CClH}^+ + \text{Cl}_2 + e^-$, fall into this category. The difference in behavior of this group of molecules was rationalized by the small size of the hydrogen atom. Extending this analysis to the CF_2X_2 series begs the obvious question of whether fragmentation of CF_2H_2^+ will behave differently to that of CF_2Cl_2^+ and CF_2Br_2^+ . The AEs of ions formed by fragmentation of CF_2Cl_2^+ and CF_2Br_2^+ are considered first. Most AEs either agree with, or are slightly in excess of, $\Delta_r H^0$ of the highest-energy process. (The one exception is the AE associated with the formation of Br^+ where, due to uncertainties in the thermochemistry, the situation is more complicated.) Hence, as with CCl_3F and CCl_3Br , fission-only processes involving loose transition states appear to dominate. The situation is slightly different with CF_2H_2 . Only one AE, associated with the formation of an ion which required the fission of more than one bond, was determined unambiguously by the TPEPICO experiment. The AE of the ion, CFH^+ , was determined to be 18.2 ± 0.4 eV. It was commented earlier that since this value was lower than $\Delta_r H^0$ associated with the highest-energy process which produces

atomic products (19.24 eV), the lower-energy reaction $\text{CF}_2\text{H}_2 \rightarrow \text{CFH}^+ + \text{HF} + e^-$ had to be involved. This process is likely to proceed via a more tightly constrained transition state, and to have a barrier along the exit channel of the potential-energy surface. As observed in the preceding paper,² for dissociation of neutral molecules as well as of ions, the hydrogenated molecule appears to behave anomalously. We rationalize this to be a steric effect caused by the small size of the hydrogen atom.

B. Determination of the dissociation dynamics from the values of $\langle \text{KE} \rangle_t$ and $\langle f \rangle_t$

The values of $\langle \text{KE} \rangle_t$ and $\langle f \rangle_t$ (Tables III, VI, and VIII) can indicate the mechanism of photodissociation of some fragmentation channels of CF_2X_2^+ . We note that the mean *total* translational kinetic-energy release, $\langle \text{KE} \rangle_t$, can only be determined for a two-body process, and its value only meaningfully interpreted if the dissociation is a single-bond fission, e.g., $\text{CF}_2\text{X}_2^+ \rightarrow \text{CF}_2\text{X}^+ + \text{X}$, and not for processes such as $\text{CF}_2\text{X}_2^+ \rightarrow \text{CFX}^+ + \text{FX}$. We have measured fixed-energy TPEPICO-TOF spectra for smaller fragment ions (e.g., CFX^+) than those reported in Tables III, VI, and VIII. Such ions can form only by multiple-bond fission, with possibly one simultaneous bond formation, and from the peak shape it is possible to determine the energy released into the fragment ion.³⁹ The data are not reported, however, since there is no simple method to infer the dissociation mechanism solely from the fragment ion kinetic energy. In this section, we only discuss the values of $\langle \text{KE} \rangle_t$ and, where the thermochemistry is known, $\langle f \rangle_t$ for reactions involving a single C–X or C–F bond fission.

First, we discuss CF_2Cl_2^+ . The values of $\langle \text{KE} \rangle_t$ and $\langle f \rangle_t$ for dissociation of CF_2Cl_2^+ to CF_2Cl^+ suggest that the \tilde{X} , \tilde{A} , \tilde{B} , and \tilde{C} states, photoionized at 12.28, 12.56, 13.19, and 13.48 eV, respectively, may dissociate by a pure-impulsive mechanism. Interestingly, there is little evidence for modified-impulsive behavior associated with the dissociation of the \tilde{X}^2B_2 and \tilde{A}^2B_1 states. This is contrary to that observed for the analogous states in CCl_3F^+ ,¹ where dissociation of the ground and first excited states was found to conform to the modified-impulsive model. The fact that the \tilde{C}^2A_1 state of CF_2Cl_2^+ dissociates by a pure-impulsive model supports the apparent selectivity of dissociation to CF_2Cl^+ , rather than to CFCl_2^+ , which is also thermochemically allowed. Despite the lack of *ab initio* calculations, Cvitas, Gusten, and Klasine¹² claim with some confidence that the \tilde{C}^2A_1 state is formed by removal of an electron from an orbital whose character is predominantly Cl lone pair. The “hole” created is, therefore, localized on the chlorine atom, which can subsequently be dispersed by rapid charge delocalization. If dissociation occurs on a time scale faster than charge redistribution, CF_2Cl^+ will selectively be formed. This selectivity can only be achieved for a rapid dissociation, hence, the observation of a value of $\langle f \rangle_t$ characteristic of a pure-impulsive process is expected. Dissociation of the \tilde{D}^2B_2 state of CF_2Cl_2^+ at 14.42 eV fits neither the pure-impulsive nor the statistical models, and appears to be a mix-

ture of the two. The difference in behavior of the \tilde{D}^2B_2 state may reflect an increase in the density of electronic states at this energy. The near-degenerate \tilde{E}/\tilde{F} states of CF_2Cl_2^+ at 16.25 eV dissociate to both CF_2Cl^+ and CFCl_2^+ . The values of $\langle \text{KE} \rangle_t$ and $\langle f \rangle_t$ (Table III) appear to indicate a competition between statistical and pure-impulsive dissociation mechanisms. Fragmentation of these states fits a statistical model for production of CF_2Cl^+ , but closer to a pure-impulsive model for production of CFCl_2^+ . The \tilde{E}^2B_1 and \tilde{F}^2A_2 states are produced by the removal of a fluorine lone-pair electron.¹² Thus, rapid-impulsive dissociation, before charge redistribution can occur, now favors C–F bond fission and production of CFCl_2^+ , whereas a statistical process should result in production of both CFCl_2^+ and CF_2Cl^+ . The experimental data seem to confirm these conclusions.

Unlike CF_2Cl_2 , the TPEPICO spectroscopy of both CF_2H_2 and CF_2Br_2 is characterized by the detection of the parent ion at low photon energies, indicating that the ground state is stable with respect to dissociation in the lower part of the Franck–Condon region. Unfortunately, accurate values for $\langle \text{KE} \rangle_t$, and hence $\langle f \rangle_t$, could not be determined for the lowest dissociation channel of CF_2H_2^+ , $\text{CF}_2\text{H}_2^+ \rightarrow \text{CF}_2\text{H}^+ + \text{H}$, due to unfavorable kinematics. Values, however, were obtained for dissociation of some of the lower valence states of CF_2H_2^+ to CFH_2^+ at photon energies of 15.31, 15.69, and 17.46 eV. The proportion of available energy channeled into translation decreases as the photon energy is increased. At 15.31 eV, the mechanism appears to be largely pure impulsive, while at 17.46 eV statistical behavior seems to dominate. This transition may reflect an increase in the density of states as the energy of excitation increases. Among the three molecules studied in this paper, CF_2H_2 has a unique electronic structure. The hydrogen atom has no lone-pair electrons so the first electron removed from the molecule originates from an orbital whose character is predominantly F lone pair. The lowest-energy dissociation channel, however, involves C–H rather than C–F bond fission. This situation, where the highest occupied molecular orbital has Y lone-pair character yet the weakest bond is C–Z (Z ≠ Y), is unique among the CF_2X_2 and CCl_3X series of molecules we have studied. For impulsive dissociation of the lower valence states of CF_2H_2^+ , we might, therefore, expect C–F bond fission to be favored, but at energies below 14.02 eV only C–H fission is thermochemically allowed. This argument predicts that the AEs of both CFH_2^+ and CF_2H^+ should be extremely close to their respective values of $\Delta_r H^0$, and that at low energies C–H bond fission should be effected by a largely statistical mechanism, while C–F bond fission should be largely impulsive. The experimental results only partially support this proposal. Dissociation to CFH_2^+ does indeed fit to an impulsive model at low energies but its AE, 14.7 eV, is ~0.7 eV above $\Delta_r H^0$. Lossing,¹⁰ however, has reported an AE of 14.06 eV which corresponds closely to the thermochemical threshold. Unfortunately, the dissociation mechanism associated with fragmentation to CF_2H^+ could not be inferred, but its AE is extremely close to the best previously determined value of $\Delta_r H^0$, as expected. In similarity with CF_2Cl_2^+ , there is little evidence for

modified-impulsive behavior associated with the dissociation of CF_2H_2^+ .

Photon-induced dissociation of CF_2Br_2^+ yields CF_2Br^+ for excitation into the \tilde{X} , \tilde{A} , \tilde{B} , \tilde{C} , \tilde{D} , and \tilde{E}/\tilde{F} states of the parent ion, and CFBr_2^+ for excitation into the degenerate \tilde{E}/\tilde{F} states. The values of $\langle \text{KE} \rangle_t$ and $\langle f \rangle_t$ determined for dissociation to CF_2Br^+ fit well to a modified-impulsive model for the \tilde{X} state; a pure-impulsive model for the \tilde{A} , \tilde{B} , and \tilde{C} states; and a statistical model for the \tilde{D} state. The observation of modified-impulsive behavior, associated with dissociation of the \tilde{X}^2B_2 state of the parent ion, is noteworthy since it was not observed for any of the valence states of CF_2Cl_2^+ or CF_2H_2^+ . This anomalous behavior may be due to the fact that the photon energy employed, 11.12 eV, is only 0.12 eV above the threshold for fragmentation. The value of E_{avail} , therefore, is much lower than in other experiments, circumstances where anomalously high values of $\langle \text{KE} \rangle_t$ can be observed.^{1,40} The trend from modified- to pure-impulsive behavior with increasing energy fits the kinematic description of the two models. The observation of statistical behavior for dissociation of the \tilde{D}^2B_2 state of CF_2Br_2^+ at 13.33 eV probably reflects the fact that the density of states and anharmonicity of molecular vibrations increases as the energy of excitation is increased. The value of $\langle f \rangle_t$ determined from the \tilde{E}/\tilde{F} states, 0.07, is extremely low and cannot be rationalized by any simple dissociation mechanism. Unfavorable kinematics prevent values of $\langle \text{KE} \rangle_t$ being determined accurately for the CFBr_2^+ TPEPICO-TOF spectra, and the lack of thermochemical data for this ion prevents any conclusions being drawn from its AE of 14.9 eV.

VI. CONCLUSIONS

Using tunable VUV radiation from a synchrotron source and TPEPICO spectroscopy, we have studied the fragmentation of the valence states of CF_2X_2^+ (X = Cl, H, Br) over the range of energies 10–25 eV. TPES, ion yield curves, and breakdown diagrams have been obtained with the experiment operating in the scanning-energy mode. In general, the peak positions in the threshold photoelectron spectra are in excellent agreement with those measured using He I radiation. A comparison of the relative intensities of the peaks indicates that the importance of autoionization producing near-threshold electrons is most pronounced in the range 14–20 eV. Autoionization is especially important in CF_2H_2 , and appears to account for a previously unobserved feature in the threshold photoelectron spectrum at 17.4 eV. The ion yields show considerable evidence of state-selective fragmentation at low energies for CF_2Cl_2^+ . The behavior of CF_2H_2^+ has not been fully characterized, and the interpretation of the ion yields from photodissociation of CF_2Br_2^+ is hampered by a lack of thermochemical data. In the cases where fragment ions can be produced by more than one dissociation channel, comparison of the appearance energy with $\Delta_r H^0$ indicates that for CF_2Br_2^+ and CF_2Cl_2^+ the highest-energy channel involving a loose transition state probably dominates. Conversely, in some circumstances CF_2H_2^+ dissociates via

lower-energy channels involving a tightly constrained transition state. The difference in behavior is rationalized by the small size of the hydrogen atom.

At fixed energy, high-resolution TPEPICO-TOF spectra have been measured for those dissociations which involve the fission of a single C–X or C–F bond. In circumstances where the kinematics are favorable and the thermochemical data are either known or can reliably be inferred, values of the mean total translational kinetic-energy release, $\langle KE \rangle_t$, and the fraction of the available energy partitioned into translation, $\langle f \rangle_t$, have been determined. The values of $\langle f \rangle_t$ are compared with those predicted for statistical, modified-impulsive, and pure-impulsive photodissociation models. In general, statistical values of $\langle f \rangle_t$ are most likely when ionization occurs at a part of the molecule furthest away from the bond that breaks. Impulsive values of $\langle f \rangle_t$ are more likely when the breaking bond lies close to the part of the molecule from which ionization occurs. Furthermore, there is a trend from impulsive to statistical behavior as the photon energy is increased. The results show clearly that these $CF_2X_2^+$ cations do not reach the ‘‘large molecule’’ limit until highly excited valence states have been attained. This behavior is extremely similar to that observed in both the CCl_3X^+ and CF_3X^+ series.^{1,38}

ACKNOWLEDGMENTS

The authors thank EPSRC, U.K. for a research grant (GR/M42794) to use the SRS, Daresbury and for studentships (D.P.S. and B.O.F.). The authors are especially grateful to Dr. G. K. Jarvis (University of Birmingham) for the use of his program to fit the fixed-energy TPEPICO-TOF spectra, and to Dr. P. A. Hatherly (University of Reading) for general advice on the use of the TPEPICO apparatus.

¹D. P. Seccombe, R. Y. L. Chim, G. K. Jarvis, and R. P. Tuckett, *Phys. Chem. Chem. Phys.* **2**, 769 (2000).

²D. P. Seccombe, R. Y. L. Chim, R. P. Tuckett, H. W. Jochims, and H. Baumgärtel, *J. Chem. Phys.* **114**, 4058 (2001), preceding paper.

³R. F. Baker and J. T. Tate, *Phys. Rev.* **53**, 683 (1938).

⁴J. W. Ajello, W. T. Huntress, Jr., and P. Rayerman, *J. Chem. Phys.* **64**, 4746 (1976).

⁵H. W. Jochims, W. Lohr, and H. Baumgärtel, *Ber. Bunsenges. Phys. Chem.* **80**, 130 (1976).

⁶H. Schenk, H. Oertel, and H. Baumgärtel, *Ber. Bunsenges. Phys. Chem.* **83**, 683 (1979).

⁷W. C. Steele, *J. Phys. Chem.* **68**, 2359 (1964).

⁸C. Lifshitz and F. A. Long, *J. Phys. Chem.* **69**, 3731 (1965).

⁹R. H. Martin, F. W. Lampe, and R. W. Taft, *J. Am. Chem. Soc.* **88**, 1353 (1966).

¹⁰F. P. Lossing, *Bull. Soc. Chim. Belg.* **81**, 125 (1972).

¹¹J. Doucet, P. Sauvageau, and C. Sandorfy, *J. Chem. Phys.* **58**, 3708 (1973).

¹²T. Cvitas, H. Gusten, and L. Klasinc, *J. Chem. Phys.* **67**, 2687 (1977).

¹³R. Jadrny, L. Karlsson, L. Mattson, and K. Siegbahn, *Phys. Scr.* **16**, 235 (1977).

¹⁴T. Pradeep and D. A. Shirley, *J. Electron Spectrosc. Relat. Phenom.* **66**, 125 (1993).

¹⁵B. P. Pullen, T. A. Carlson, W. E. Moddeman, G. K. Schweitzer, W. E. Bull, and F. A. Grimm, *J. Chem. Phys.* **53**, 768 (1970).

¹⁶C. R. Brundle, M. B. Robin, and H. Basch, *J. Chem. Phys.* **53**, 2196 (1970).

¹⁷A. W. Potts, H. J. Lempka, D. G. Streets, and W. C. Price, *Philos. Trans. R. Soc. London, Ser. A* **268**, 59 (1970).

¹⁸J. Doucet, R. Gilbert, P. Sauvageau, and C. Sandorfy, *J. Chem. Phys.* **62**, 366 (1975).

¹⁹T. Cvitas, H. Gusten, L. Klasinc, I. Novak, and H. Gusten, *Int. J. Quantum Chem., Quantum Chem. Symp.* **14**, 305 (1980).

²⁰I. Novak, J. M. Benson, and A. W. Potts, *Chem. Phys.* **104**, 153 (1986).

²¹W. Kischlat and H. Morgner, *J. Electron Spectrosc. Relat. Phenom.* **35**, 273 (1985).

²²P. A. Hatherly, M. Stankiewicz, K. Codling, J. C. Creasey, H. M. Jones, and R. P. Tuckett, *Meas. Sci. Technol.* **3**, 891 (1992).

²³P. A. Hatherly, D. M. Smith, and R. P. Tuckett, *Z. Phys. Chem.* **195**, 97 (1996).

²⁴W. C. Wiley and I. H. Maclaren, *Rev. Sci. Instrum.* **26**, 1150 (1955).

²⁵G. K. Jarvis, D. P. Seccombe, and R. P. Tuckett, *Chem. Phys. Lett.* **315**, 287 (1999).

²⁶M. W. Chase, *J. Phys. Chem. Ref. Data Monogr.* **9** (1998).

²⁷S. G. Lias, J. E. Bartmess, J. F. Liebman, J. L. Holmes, R. D. Levin, and W. G. Mallard, *J. Phys. Chem. Ref. Data Suppl.* **17**, 1 (1988).

²⁸S. G. Lias and P. Ausloos, *Int. J. Mass Spectrom. Ion Phys.* **23**, 273 (1977).

²⁹R. J. Blint, T. B. McMahon, and J. L. Beauchamp, *J. Am. Chem. Soc.* **96**, 1269 (1974).

³⁰T. Ibuki, A. Hiraya, and K. Shobatake, *J. Chem. Phys.* **90**, 6290 (1989).

³¹G. H. Wannier, *Phys. Rev.* **90**, 817 (1953).

³²F. T. Prochaska and L. Andrews, *J. Chem. Phys.* **68**, 5577 (1978).

³³K. Takeshita, *Chem. Phys. Lett.* **165**, 232 (1990).

³⁴D. H. Rank, E. R. Shull, and E. L. Pace, *J. Chem. Phys.* **18**, 885 (1950).

³⁵J. L. Franklin, P. M. Hierl, and D. A. Whan, *J. Chem. Phys.* **47**, 3184 (1967).

³⁶L. Andrews, J. M. Dyke, N. Jonathan, N. Keddar, A. Morris, and A. Ridha, *J. Phys. Chem.* **88**, 2364 (1984).

³⁷F. T. Prochaska and L. Andrews, *J. Phys. Chem.* **82**, 1731 (1978).

³⁸J. C. Creasey, D. M. Smith, R. P. Tuckett, K. R. Yoxall, K. Codling, and P. A. Hatherly, *J. Phys. Chem.* **100**, 4350 (1996).

³⁹J. Mähner, H. Baumgärtel, and K. M. Weitzel, *J. Chem. Phys.* **102**, 180 (1995).

⁴⁰P. Downie and I. Powis, *J. Chem. Soc. Faraday Disc.*, **115**, 103 (2000).